Korean J. Chem. Eng., **14**(6), 451-458 (1997)

EFFECT OF METAL/ACID BALANCE IN Pt-LOADED LARGE PORE ZEOLITES ON THE HYDROISOMERIZATION OF *n*-HEXANE AND *n*-HEPTANE

Jeong-Kyu Lee and Hyun-Ku Rhee†

Department of Chemical Engineering, Seoul National University, Kwanak-ku, Seoul 151-742, Korea
(*Received 18 September 1997 • accepted 21 November 1997*)

Abstract – Large-pore zeolites H-Beta, H-Mordenite and H-Omega were loaded with platinum and applied for the hydroisomerization of *n*-hexane and *n*-heptane. The catalytic activity of Pt-loaded zeolite showed good correlation with the effective acidity probed by pyridine rather than with the total acidity probed by ammonia when equal amounts of metal sites are present. The selectivity to multibranched isomers over three different catalysts was found dependent upon the conversion of *n*-paraffin. At low conversion, the selectivity to multibranched isomers was higher over Pt-loaded zeolites with high acid strength. At high conversion level, however, the selectivity was mainly governed by the metal/acid balance. On H-Mordenite and H-Omega, large amount of strong acid sites are located in the small pore or cage. In Pt/H-MOR, the metal/acid balance was poor because there was detrimental loss of metal sites caused by isolation of Pt in the side pockets of 8-MR and/or pore blockage of the linear 12-MR channel. Even though the acidity of H-Beta was very low compared to H-MOR and H-Omega, Pt/H-Beta yielded the best performance for the hydroisomerization of *n*-paraffin because of better metal/acid balance in Pt/H-Beta.

Key words: Pt/Zeolite, Hydroisomerization, n-Hexane, n-Heptane, Metal/Acid Balance

INTRODUCTION

Bifunctional Pt/zeolite catalyst plays an important role in processes such as hydrocracking, isomerization and catalytic dewaxing [Maxwell and Stork, 1990]. The activity of bifunctional Pt/zeolite catalyst and the selectivity of *i*-paraffins are strongly influenced by the numbers of acid and metal sites [Guisnet and Perot, 1984]. The optimum performance of Pt/H-Y with respect to hydroisomerization of *n*-heptane was obtained when the ratio of strong acid sites to metal sites is below 6 [Giannetto et al., 1986; Alvarez et al., 1987]. In the Pt/H-Y catalysts, the number of strong acid sites was characterized by the heat of adsorption of ammonia exceeding 100 kJ/mol and the number of metal sites by hydrogen chemisorption. In this case, all the strong acid sites including those located in small pore or cage will be counted irrespective of the fact that those acid sites cannot participate in the transformation of bulky carbenium ions. And the distribution as well as the dispersion of metal might be characterized differently due to the structure of zeolites in which platinum particles are dispersed [Lee and Rhee, 1997]. Therefore, the distribution as well as the numbers of acid and metal sites should be taken into account for platinum loaded zeolites having different structures.

In this study, 12-MR large-pore zeolites with various Si/Al ratios were synthesized and loaded with platinum, and then applied for the hydroisomerization of *n*-paraffin. Especially, we were concerned with the distribution of acid and metal sites in Pt-loaded zeolites and the effect of metal/acid balance on the hydroisomerization of *n*-paraffin was discussed. Finally, the difference in activity among Pt/H-MOR, Pt/H-Omega and Pt/H-Beta was discussed in detail.

†To whom all correspondence should be addressed.
E-mail: hkrhee@plaza.snu.ac.kr

EXPERIMENTAL

1. Catalyst Preparation

Zeolite Beta was synthesized hydrothermally in a Teflon-lined autoclave from Na_2O-SiO_2-Al_2O_3-$(TEA)_2O$-H_2O system using tetraethylammonium hydroxide (TEAOH) as template [Wadlinger et al., 1967; Leu et al., 1991]. Zeolite Omega was synthesized according to the procedure reported by Nicolas et al. [1988]. The structure of synthesized zeolite Omega and Beta were analyzed by XRD and FTIR spectroscopy and the results were found to match well with those reported earlier [Wadlinger et al., 1967; Leu et al., 1991; Nicolas et al., 1988]. The as-synthesized zeolites were calcined in air at 550 °C and ion exchanged with 1 M $(NH_3)_4Cl$ three times at 80 °C under reflux. H-Beta and H-Omega were obtained by calcination of $(NH_3)_4$-zeolite in air at 540 °C.

Steaming at high temperatures and subsequent acid leaching procedures were applied for H-Omega to dealuminate parent H-Omega. Typically, 1.0 g of H-Omega was loaded in a quartz reactor and was heated up to 600 °C or 700 °C in air flow (20 cc/min). And steam (P_{H_2O}=37.1 kPa) was directed into the reactor at the planned temperatures for 2 hr. The steamed samples were treated with HNO_3 solution (300 cc/g-zeolite) of various concentrations (0.05, 0.1 and 0.2 N HNO_3) at 80 °C under reflux for 12 hr. The dealuminated samples were designated as OMSA-1 (steaming at 600 °C, leaching with

Table 1. Summary of platinum-loaded zeolite preparation

Catalyst	Pt (wt%)	Si/Al ratio	Method
Pt/H-MOR	0.5	22.5	IE
	0.5	6.5	IE
	2.0	6.5	IE
Pt/H-Beta	0.5	12.5	IWI
	0.5	12.5	IE
	0.5	15.4	IWI
	2.0	15.4	IWI
	0.5	37.5	IWI
Pt/H-Omega	0.5	5.6	IWI
Pt/OMSA-1	0.5	36.7	IWI
Pt/OMSA-2	0.5	48.6	IWI
Pt/OMSA-3	0.5	10.8	IWI

IE: Ion-exchange, IWI: Incipient Wetness Impregnation.

0.1 N HNO_3), OMSA-2 (600 °C, 0.2 N) and OMSA-3 (700 °C, 0.2 N). H-MOR were taken from commercial samples (PQ Corp., SiO_2/Al_2O_3=13.0, 25 and 45) and commercial zeolite Beta's (PQ Corp., SiO_2/Al_2O_3=25 and 75) were also used. The Si/Al ratios of synthesized H-Beta and H-Omega were analyzed by ICP-AES and EDX.

Platinum loaded zeolites were prepared by both the ion-exchange and the incipient wetness impregnation methods using $[Pt(NH_3)_4]Cl_2$ as precursor. Platinum loaded catalysts were dried at 110 °C overnight and then heated at a rate of 0.5 °C/min in O_2 flow (1 *l*/min·g-cat) up to various calcination temperatures T_c (200, 300, 350, 400 and 500 °C). The catalysts were maintained at each of these temperatures for 2 hr and allowed to cool down to the room temperature in He flow. Reduction was then performed in H_2 flow (200 cc/min·g-cat) by raising the temperature at a rate of 2 °C/min to 500 °C and the temperature was held at 500 °C for 1 hr. The catalysts examined in this study are summarized in Table 1.

2. Catalyst Characterization

For temperature programmed desorption (TPD) of ammonia and pyridine, the bed of H-form zeolite (0.1 g) was heated at 500 °C in He flow for 1 hr. Ammonia or pyridine was introduced in He flow into the bed after cooling the bed to 100 °C or 200 °C, respectively. The TPD was started by increasing the temperature at a rate of 15 °C/min. The desorbed ammonia and pyridine was detected by TCD and an interfaced computer was used for data recording.

To investigate the structural changes of dealuminated zeolite Omega samples, ^{27}Al MAS NMR spectra were obtained on a Bruker ARX300 MAS spectrometer. ^{27}Al NMR spectra were recorded at 78.3 MHz with radiofrequency pulses of 2.8 μs. A number of 1,000 free induction decays were accumulated per sample at a repetition time of 1 s. $Al(OH_2)_6^{3+}$ was used as external reference to measure the chemical shifts.

For FTIR study of CO adsorbed catalysts, self-supporting wafers of Pt/H-Beta and Pt/H-MOR were pretreated *in-situ* under the same operation conditions as mentioned above in a glass cell which was fitted with NaCl windows and high-vacuum stopcocks. Afterwards, the cell was evacuated to a pressure of approximately 10^{-2}-10^{-3} Torr and cooled down to room temperature (RT). The samples were then exposed to CO at 20 Torr for 15 min. The spectrum was recorded after evacuation to the base pressure at room temperature and 100 °C, respectively, for 15 min.

Hydrogen chemisorption was performed in a static vacuum volumetric apparatus at RT to investigate metal dispersion. The detailed procedure was described elsewhere [Lee et al., 1996]. For EXAFS measurements, pretreated samples of 200-250 mg were pressed into self-supporting wafers (10 mm diameter). The samples calcined at different temperatures were reduced at 500 °C as described above. These samples were reduced again in H_2 flow at 573 K using a Pyrex U-tube reactor and transferred to an EXAFS cell with Kapton (Du Pont, 125 μm) windows. The cell was sealed off under H_2 with flame. The EXAFS was measured using Beam Line 10B at the Photon Factory in Tsukuba in the transmission mode at the Pt L_{III} at room temperature. A Si(311) channel cut monochromator was used and the resolution ($\Delta E/E$) was 1×10^{-4}. The X-ray energy was increased by 2.2 eV steps. The X-ray intensity was measured by using gas ionization chambers. X-ray absorption data was analyzed by standard methods using the UWXAFS 2.0.

3. Reaction Experiment

The reaction experiment was conducted in a fixed-bed down-flow reactor with H_2/*n*-paraffin molar ratio of 6.0 under the atmospheric pressure. *n*-Paraffin (purity>99.5 %) was fed to the reactor in H_2 flow by a microfeeder. To investigate the hydrogenation activities of platinum-loaded zeolite catalysts, the hydrogenation of benzene was also conducted at 100 °C with H_2/benzene molar ratio of 9.8 and WHSV=29.3 hr^{-1} under the atmospheric pressure. The product was analyzed by using a GC-FID fitted with HP-PONA (crosslinked methylsilicone, 50 m×0.2 mm×0.5 μm) capillary column.

RESULTS AND DISCUSSION

1. Acidity and Acid Sites Distribution in Zeolites

The acidities of zeolites were examined by using ammonia and pyridine as probe molecules. The amount of strong acid sites of various zeolites probed by ammonia and pyridine, respectively, are given in Table 2 and they are plotted against Si/Al ratio of zeolites in Fig. 1. From the results of ammonia TPD, it is evident that the strength and amount of strong acid sites were largest on H-Omega among three different zeolites (Table 2). The acidity of H-Beta turned out to be lowest. When pyridine was used as probe basic molecules, however, the acidity of H-Beta was largest among three zeolites as shown in Table 2.

The amount of acid sites measured by ammonia TPD decreases as the Si/Al ratio increases. But the amount of strong acid sites does not show linear dependence on Al content. The amount measured by pyridine TPD, however, was rather independent of the Si/Al ratio of different type zeolites. These results suggest that large amount of acid sites are inaccessible to pyridine with molecular size of about 5.85 Å in H-MOR and H-Omega while ammonia can have access to almost all the acid sites in microporous zeolites.

The amount of strong acid sites of OMSA-n (n=1,2,3) series substantially decreased compared to that of parent H-

Table 2. Acidic properties of various zeolites

Zeolites (Si/Al ratio)	NH_3 desorbed (mmol/g-cat)		Pyridine desorbed (μmol/g-cat)	
	LT-peak[a] (T_m, °C)[e]	HT-peak[b] (T_m, °C)	LT-peak[c] (T_m, °C)	HT-peak[d] (T_m, °C)
H-MOR				
(6.5)	0.63 (230)	0.48 (550)	12.71 (305)	10.52 (620)
(22.5)	0.24 (230)	0.24 (680)	11.62 (285)	51.61 (685)
H-Beta				
(12.5)	0.53 (220)	0.31 (320)	17.31 (303)	41.62 (595)
(15.4)	0.44 (225)	0.29 (375)	19.23 (320)	33.02 (-)
(37.5)	0.19 (210)	0.23 (390)	6.03 (265)	24.82 (685)
H-Omega (5.6)	1.05 (225)	0.73 (575)	7.67 (305)	14.44 (-)
OMSA-1 (36.7)	0.30 (210)	0.18 (375)	nd	nd
OMSA-2 (48.6)	0.16 (195)	0.19 (520)	nd	nd
OMSA-3 (10.8)	0.46 (220)	0.36 (-)	32.96 (285)	15.75 (-)

[a]Ammonia desorbed at 100-325 °C, [b]Ammonia desorbed above 325 °C, [c]Pyridine desorbed at 200-400 °C, [d]Pyridine desorbed above 400 °C, [e]Maximum desorption temperature in °C.

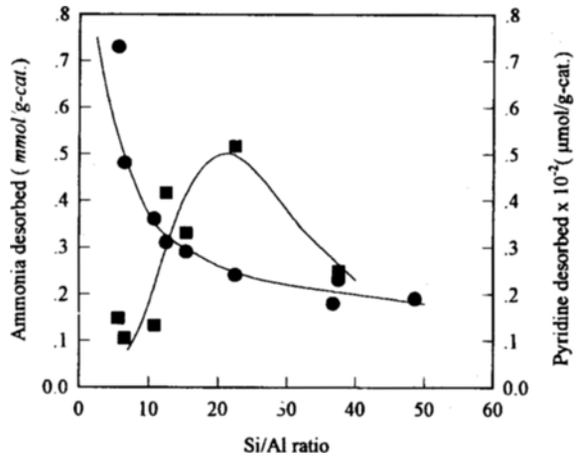

Fig. 1. Amounts of ammonia (●) and pyridine (■) desorbed at high temperature vs. Si/Al ratio of various zeolites.

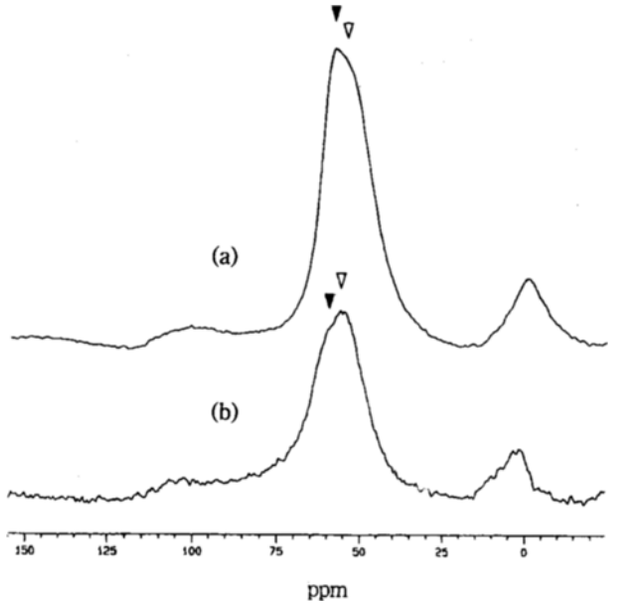

Fig. 2. ^{27}Al MAS NMR spectra of (a) H-Omega and (b) OMSA-3.

Omega when ammonia was used as probe molecule. On the other hand, the acidity of OMSA-3 was higher than that of parent H-Omega when probed by pyridine. This result indicates that the zeolite Omega tends to have more open structure and there exist more acid sites accessible to pyridine even though the Al content decreases by dealumination.

2. ^{27}Al MAS NMR Spectra

^{27}Al MAS NMR spectra of parent H-Omega and dealuminated OMSA-3 are presented in Fig. 2. Two resonance lines are observed at 55 ppm and 0 ppm. The peak at 55 ppm corresponds to the tetrahedrally coordinated Al of the lattice and the additional peak at 0 ppm to octahedral Al species extracted from the lattice. In the parent H-Omega, some of Al exists as octahedral species. It is understood that during the calcination of as-synthesized and NH_4-form zeolite Omega, some of the lattice Al could be extracted out of framework as octahedral Al species before dealumination procedure. The amount of Al in the framework of zeolite Omega decreased in OMSA-3 compared to the parent H-Omega.

A close examination of the resonance peak around 55 ppm reveals that there are two crystallographically non-equivalent Al sites. The framework of zeolite Omega contains two different Al sites, site A and site B, which are located in the 4-MRs (4-membered rings) of the gmelinite cages (S4R) and in the 6-MR (S6R), respectively[Klinowski and Anderson, 1986; Massiani et al., 1988]. In the NMR spectra of parent H-Omega, the peak at higher ppm is more intense but the peak at lower ppm became more intense in OMSA-3. The peak at higher ppm was assigned to Al in S4Rs and that at lower ppm to Al in S6Rs [Buckermann et al., 1993]. Therefore, Al in the S4Rs of gmelinite cages are more easily extracted than that in S6Rs. These results lead us to the deduction that the linear channel of 12-MR could be partially destroyed to have more open structure and the Al sites deep in the S6Rs could be exposed to the main channel of 12-MR by preferential dealumination in S4Rs near main channel.

3. H_2/CO Chemisorption and EXAFS Results

The H/Pt values obtained from H_2 chemisorption for Pt/H-MOR and Pt/H-Beta are plotted against the calcination tem-

perature in Fig. 3. The catalysts are reduced at 500 °C for 1 hr. The maximum value of H/Pt was obtained when T_c=350 °C for Pt/H-MOR or T_c=300 °C for Pt/H-Beta. When the catalysts were calcined at temperatures below 400 °C, all the catalysts had H/Pt value greater than the assumed stoichiometric value of 1.0.

The EXAFS results are given in Table 3. The nearest neighbor coordination numbers (CN) of platinum clusters in Pt/H-MOR are below 6, which corresponds to the average diameters of spherical platinum clusters of below 10 Å [Shpiro et al., 1991]. In the case of Pt/H-Beta, CN values are in the range of 8.1-9.5 depending on the calcination temperatures. These CN values correspond to spherical platinum clusters of below 15 Å in diameter which could possibly be located in the channel intersections of zeolite Beta. The particle size of Pt in Pt/H-MOR is smaller than that of Pt in Pt/H-Beta probably because Pt/H-MOR was prepared by ion-exchange while Pt/H-Beta by impregnation method.

For both catalysts, there exist optimum calcination temperatures. In accordance with previous pretreatment studies of Pt/Y zeolites [Homeyer and Sachtler, 1986] and Pt/ZSM-5 [Folefoc and Dwyer, 1992], the calcination temperature should be high enough to decompose the amine ligands of Pt precursor otherwise mobile neutral Pt species which accelerate agglomeration of Pt could be formed. When the calcination temperature increased, on the other hand, most of Pt^{2+} ions probably migrate into small pore [Chmelka et al., 1989] or near pore mouths. Upon reduction at 500 °C, metal atoms gradually migrate to the external surface of the zeolite, where they could form large particles.

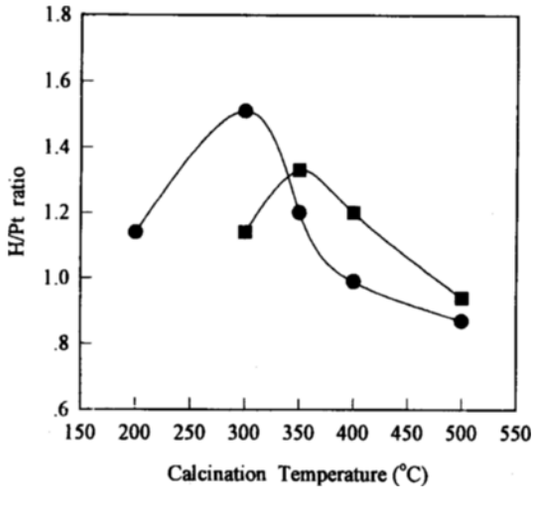

Fig. 3. H/Pt ratios of Pt/H-MOR (■) and Pt/H-Beta (●) catalysts calcined at various temperatures.

Table 3. EXAFS parameters and CO/Pt ratios for Pt/H-MOR and Pt/H-Beta after different treatments

Catalysts	N[a]	R (Å)[b]	$\triangle\sigma^2$ (Å^2)[c] × 100	CO/Pt
M300[d]	5.7	2.72	0.81	0.40
M350	5.9	2.72	0.85	0.44
B200[e]	9.5	2.76	0.57	0.21
B300	8.1	2.75	0.65	0.31
B500	8.9	2.75	0.67	0.40

Note; All catalysts were loaded with 2.0 wt% Pt and were reduced at 500 °C for 1 hr.
[a]Pt-Pt coordination number (±0.3).
[b]Pt-Pt coordination distance (±0.001).
[c]The Debye-Waller factor (±0.04).
[d]Calcination temperature (°C) of 2.0 wt% Pt/H-MOR.
[e]Calcination temperature (°C) of 2.0 wt% Pt/H-Beta.

The CO/Pt ratios obtained from CO chemisorption are also given in Table 3. Compared to the CN values, the CO/Pt ratios from Pt/H-MOR are not so much higher than those from Pt/H-Beta. For example, the CO/Pt ratio from B500 is the same as that from M300 even though CN value from M300 is much smaller than that from B500. This implies that some of Pt particles in Pt/H-MOR are inaccessible to CO. The catalysts listed in Table 3 contained 2.0 wt% of Pt. Since the growth of particles would be accelerated by the amount of metal loading [Homeyer and Sachtler, 1989], the average diameters of Pt particles in Pt/H-MOR and Pt/H-Beta loaded with 0.5 wt% Pt are expected to be smaller than that in catalysts loaded with 2.0 wt% Pt. Therefore, Pt particles must be well dispersed in the channels of both zeolites.

4. *In-situ* CO-IR

The infrared spectra of CO adsorbed on Pt/H-MOR are presented in Fig. 4. At saturation coverage, three bands were observed at 2,124, 2,087 and 1,867 cm^{-1}, respectively. The intense peak at 2,087 cm^{-1} was assigned to the linear CO band while the small band at 1,867 cm^{-1} to the bridging CO band. As shown in Fig. 4, the absorbance of the band at 2,124 cm^{-1} increased with T_c. The peak location suggests that this platinum species was in a low positive oxidation state. Some authors [Zholobenko et al., 1994; Otten et al., 1994; Stakheev et al., 1997] assigned this peak to CO adsorbed on very small clusters or monatomic Pt^I monocarbonyl species. The peak position of linear CO band shifted to the lower wave number by 10 cm^{-1} when the sample was evacuated at 100 °C instead of at RT. The peak position of band at 2,124 cm^{-1}, however, was unaffected by CO coverage. This indicates that CO species observed at 2,124 cm^{-1} had little interaction with neigh-

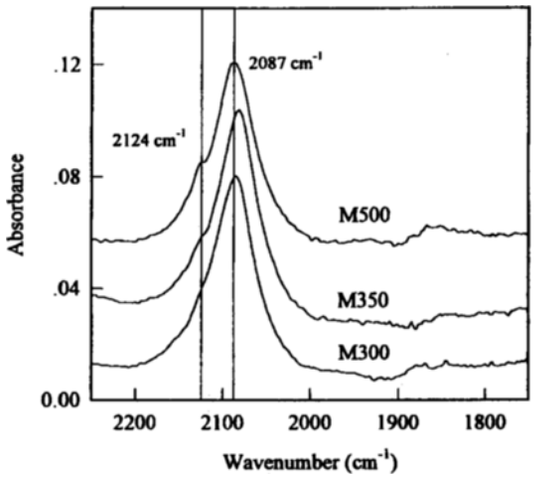

Fig. 4. Infrared spectra of CO adsorbed on Pt/H-MOR catalysts calcined at various temperatures.

boring CO and thus the clusters serving as adsorption sites for CO were associated with isolated Pt species in H-MOR channel. Mortier [1977] determined Ca^{+2} ion sites in CaMOR to show that the sites deepest in the side-pockets of 8-MR are preferentially occupied and the sites in the main channel of 12-MR were the second in population and stability of the cations at high temperature above 350 °C. Mortier suggested that the favorable coordination of bipositive ions with oxygen ions would be the reason for the stability of Ca^{+2} ions in the side-pockets.

The infrared spectroscopy of CO adsorbed on Pt/H-MOR and Pt/H-Beta calcined at 350 °C are presented in Fig. 5. The intensity of band at 2,124 cm^{-1} on Pt/H-MOR is much more intense than that on Pt/H-Beta. There might be two explanations for this result. One is that the proton concentration which interacts with Pt atoms is high in H-MOR because the Si/Al ratio of H-MOR is lower than that of H-Beta. The other is that Pt atoms could be isolated in the side pockets of 8-MR in H-MOR, while all the channels of H-Beta are composed of 12-MR.

Therefore, the increase in absorbance of band at 2,124 cm^{-1} with T_c may be regarded as an evidence that Pt^{+2} ions initially located in the main channel might have migrated into the side-pockets. After the reduction step, some of Pt clusters still remain in the side-pockets, where Pt clusters interact with H^+ to have electron deficient character. Therefore, it is reasonable to assign the band at 2,124 cm^{-1} to CO adsorbed on isolated Pt clusters in the side-pockets of mordenite channel.

5. Activity of Platinum-loaded Zeolites

In Fig. 6, the conversion of *n*-hexane over platinum-loaded (0.5 wt%) zeolite catalysts are plotted against the amount of strong acid sites probed by ammonia and pyridine given in Table 2. As shown in Fig. 6(a), the catalytic activity of bifunctional Pt/zeolite showed maximum when the amount was around 0.3 mmol/g-cat. This amount of strong acid sites would correspond to the ratio of acid sites to metal sites of 1.2 if the metal dispersion is 1.0. This value of the ratio is sufficient enough to be a good hydroisomerization catalyst according to the study by Gianneto et al. [1986] and Alvarez et al. [1987].

The catalytic activities of various Pt-loaded zeolites for the hydroisomerization of *n*-hexane is presented in Fig. 6(b) with the strong acid sites determined by pyridine TPD instead of ammonia. In contrast to the strong acid sites determined from ammonia, the conversion increased with the strong acid sites determined from pyridine. If the molecular sizes of mono- (>5 Å) and di-brached isoalkenes (> 6 Å) are taken into account, the acid sites which are inaccessible to pyridine could not serve as adsorption sites for relatively large reaction intermediates. When the number of acid sites is obtained by ammonia, the acid sites which could not participate in the transformation of bulky iso-carbocations might be counted. As shown in Fig. 6(a), the activity decreased again when acid/metal ratio decreased from the optimum ratio. For all the zeolites, however, the ratio of acid sites determined from pyridine to those determined from ammonia is below 0.2 because TPD was run after adsorption of probe molecules under flowing condition. For more rigorous analysis, adsorption of probe molecules under vacuum is recommended.

The results from hydroisomerization of *n*-hexane over Pt-loaded zeolite catalysts are listed in Table 4. The catalytic activity and the yield of *i*-C_6 were highest over Pt/H-Beta. The activity of Pt/H-Omega is very low compared to those of Pt/H-MOR and Pt/H-Beta though the acidity and the ef-

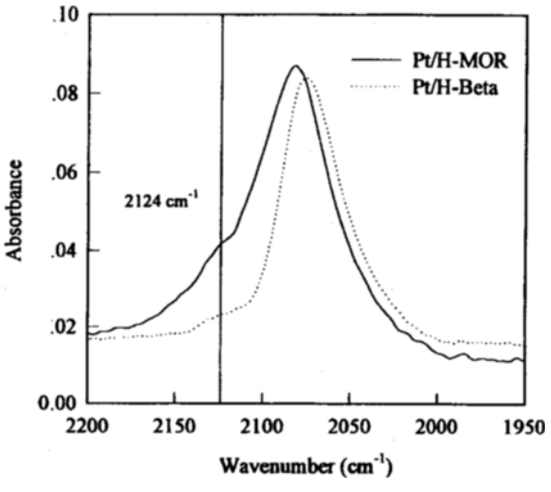

Fig. 5. Infrared spectra of CO adsorbed on Pt/H-Beta and Pt/H-MOR catalysts calcined at 350 °C.

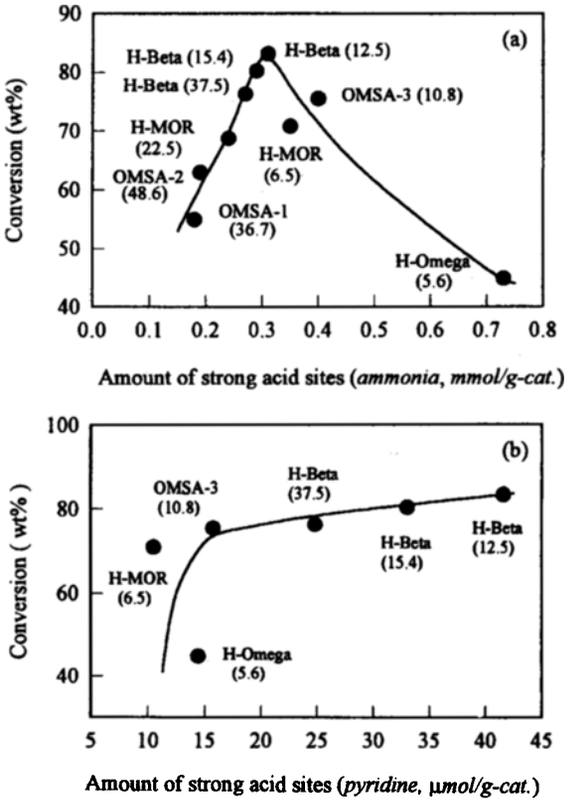

Fig. 6. Conversion of *n*-hexane vs. the amount of strong acid sites determined from (a) ammonia and (b) pyridine over various Pt/zeolite catalysts (WHSV=1.58 hr^{-1}, H_2/*n*-hexane=6.0, 280 °C). Numbers inside the parentheses denote the Si/Al ratio.

Table 4. Product distributions from hydroisomerization of *n*-hexane over Pt-loaded zeolite catalysts

Catalysts (Si/Al ratio)	Conversion (%)	Product composition, wt%				Σi-C_6	i-C_6 selectivity (%)
		C_1-C_5	ΣDMB[a]	2-MP[b]	3-MP[c]		
Pt/H-MOR							
(6.5)	70.7	1.2	13.9	33.8	21.8	69.5	98.3
(12.5)	74.3	3.5	15.0	33.2	22.6	70.8	95.3
(22.5)	68.7	9.5	12.0	28.8	18.4	59.2	86.2
Pt/H-Beta							
(12.5)	83.1	5.9	23.8	32.3	21.2	77.3	92.9
(15.4)	80.2	3.2	23.7	33.3	21.7	78.7	96.1
(37.5)	76.2	1.0	15.9	36.3	23.1	75.3	98.7
Pt/H-Omega	44.8	6.0	7.2	19.1	12.6	38.9	86.6
Pt/OMSA-1	54.9	1.7	7.3	26.7	17.9	51.9	94.6
Pt/OMSA-2	62.9	3.0	10.1	30.8	20.3	61.2	97.2
Pt/OMSA-3	75.4	7.1	14.2	32.8	21.2	68.2	90.5

Notes; Reaction conditions: WHSV=1.58 hr^{-1}, H_2/*n*-hexane=6.0, temp.= 280°C, total pressure=1 atm. All catalysts were loaded with 0.5 wt% Pt.

[a]2,3-Dimethylbutane+2,2-Dimethylbutane, [b]2-Methylpentane, [c]3-Methylpentane.

Table 5. Product distributions from hydroisomerization of *n*-heptane over Pt/H-Beta and Pt/H-MOR catalysts at various temperatures

Catalyst	Pt/H-Beta			Pt/H-MOR		
Temp. (°C)	260	270	300	240	260	270
Product (wt%)						
C_6^-	5.6	19.2	61.6	1.9	14.4	33.4
(%i-C_4)	(39.3)	(52.1)	(51.5)	(52.6)	(54.2)	(54.2)
ΣMono-[a]	48.6	46.3	21.1	24.0	35.5	30.8
ΣMulti-[b]	14.2	20.2	11.6	5.4	12.1	11.7
Conv. (wt%)	68.4	85.7	94.3	31.3	62.0	75.8
i-C_7 yield (wt%)	62.8	66.5	32.7	29.4	47.6	42.4
i-C_7 selec. (%)	91.8	77.6	34.6	93.8	76.8	56.0
△ RON (C_5^+)	38.2	49.9	56.3	16.7	32.9	38.7

Notes; Reaction conditions: H_2/*n*-Heptane=6.0, WHSV=1.639 hr^{-1}, Total pressure=1 atm.

[a]Methylhexanes+Ethylpentane.

[b]Dimethylpentanes+Trimethylbutane.

fective pore size of H-Omega are largest. When H-Omega was subjected to dealumination under various conditions, the activity was considerably increased. The acidity determined from ammonia of OMSA-n series substantially decreased compared to the parent H-Omega as given in Table 2. On the other hand, the acidity probed by pyridine was higher on OMSA-3 than that on H-Omega. Over Pt/OMSA-3, the catalytic activity and the yield of i-C_6 were comparable to those over Pt/H-MOR while Pt/H-Omega (5.6) showed very low activity.

Presented in Table 5 are the product distributions from hydroisomerization/hydrocracking of *n*-heptane over Pt/H-MOR and Pt/H-Beta. The maximum yields of i-C_7 over Pt/H-Beta and Pt/H-MOR are 66.5 wt% and 47.6 wt%, respectively. The yield of multibranched isomers is much higher over Pt/H-Beta than that over Pt/H-MOR. In the cracked product, i-C_4 (i-butane) is above 50 mole% over both catalysts.

6. Selectivity to Multibranched Isomers

Both the catalytic activity and the selectivity to multibranched isomers were highest on Pt/H-Beta as given in Table 4 and 5. However, the selectivity was not always higher over Pt/H-Beta. In Fig. 7 the selectivity to multibranched isomers from hydroisomerization of *n*-hexane [Part (a)] and *n*-heptane [Part (b)] are plotted against the contact time and the conversion. At low conversion (or low contact time), the selectivity was higher over Pt/H-MOR because of the higher strength of acid sites in H-MOR. The selectivity over Pt/H-Beta increased rapidly with conversion to become higher than that over Pt/H-MOR at high conversion. As the conversion increases, the residence time of carbenium ions on acid site would become much larger, and then the metal/acid balance in Pt/zeolite seems to play an important role for the high selectivity to multibranched isomers.

7. Effect of Pretreatment Conditions

Pt/H-Beta and Pt/H-MOR were prepared under various pretreatment conditions and applied for the hydroisomerization of *n*-hexane and *n*-heptane. The catalytic activities of Pt/H-MOR and Pt/H-Beta for the hydroisomerization of *n*-hexane are plotted against the calcination temperature in Fig. 8(a) and also against the reduction temperature in Fig. 8(b). Clearly, the catalytic activity of bifunctional Pt/zeolite strongly depends on the activation temperatures. The highest activity was obtained with the catalysts calcined at 300-350 °C and subsequently reduced at 500 °C. Since the acidities of both Pt/H-MOR and Pt/H-Beta are unaffected by the thermal activation conditions adopted in this study, the activity variation must be caused by the change in metallic centers.

The activities of Pt/H-MOR and Pt/H-Beta for the hydroisomerization of *n*-hexane are plotted against the H/Pt value (Pt dispersion) in Fig. 9. When the H/Pt value was low, the activity increased with H/Pt and then approached to a limiting value as H/Pt increased. For identical value of H/Pt, the activity of Pt/H-Beta was higher than that of Pt/H-MOR and the difference in activity became larger as H/Pt increased. Since the number of metal sites are identical in both catalysts, the acidity and the distribution of Pt clusters in zeolite channels should be responsible for the difference in activity.

To compare the hydrogenation activity between Pt/H-MOR and Pt/H-Beta, the hydrogenation of benzene was conducted. The hydrogenation activity of Pt/H-Beta (TOF=30-100 s^{-1})

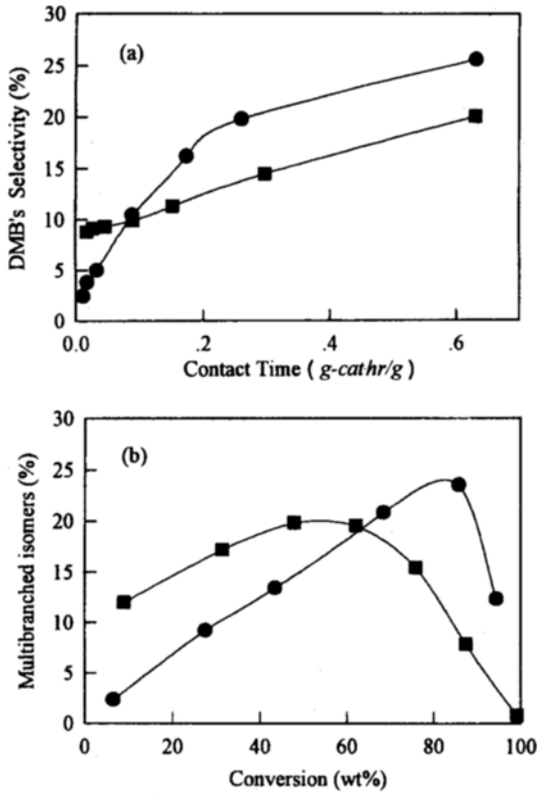

Fig. 7. Selectivities of DMB's and multibranched isomers from hydroisomerization of *n*-hexane (a) *n*-heptane (b) over Pt/H-Beta (●) and Pt/H-MOR (■) catalysts (WHSV= 0.66-59.4 h^{-1} at 270 °C for *n*-hexane conversion, WHSV= 1.58 h^{-1} at 220-300 °C for *n*-heptane conversion).

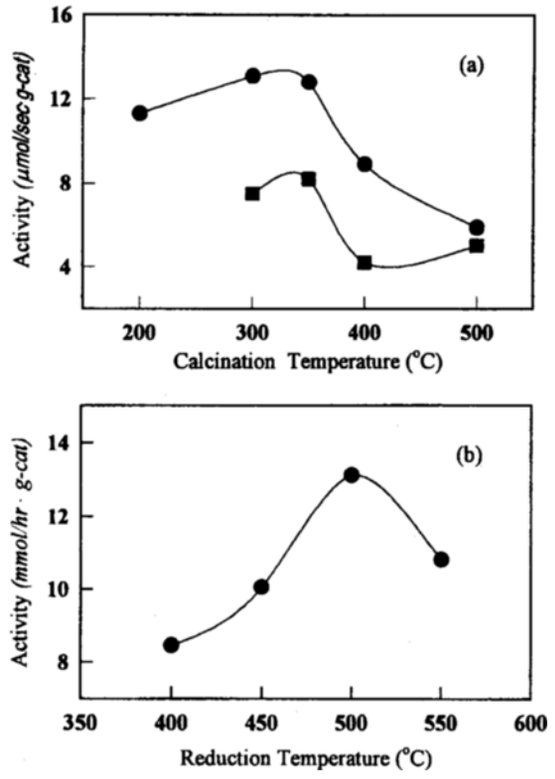

Fig. 8. Activities of Pt/H-Beta (●) and Pt/H-MOR (■) for the hydroisomerization of *n*-hexane vs. (a) calcination temperature and (b) reduction temperature (WHSV=9.9 h^{-1}, H_2/*n*-hexane=6.0, 270 °C).

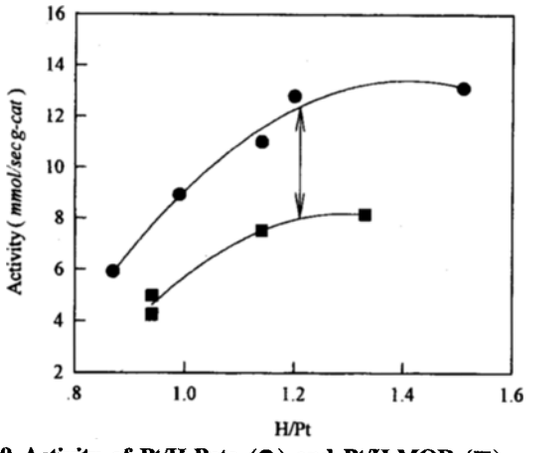

Fig. 9. Activity of Pt/H-Beta (●) and Pt/H-MOR (■) vs. H/Pt ratio for the hydroisomerization of *n*-hexane (WHSV= 9.9 h^{-1}, H_2/*n*-hexane 6.0, 270 °C).

was extremely high in comparison to that of Pt/H-MOR (TOF= 0.4-2.7 s^{-1}) when the Pt dispersion was about the same for both catalysts. If most of the Pt clusters are located on the outer surface of the zeolite crystallites, the hydrogenation activities of both catalysts would be similar. Therefore, the large difference in hydrogenation activity between the two catalysts might be attributed to the difference in the number of Pt clusters exposed to benzene or the accessibility of benzene to the Pt clusters in the zeolite channels. As discussed on the EXAFS results and CO/Pt values, large amount of Pt clusters in Pt/H-MOR are inaccessible to CO and benzene although they are highly dispersed in the channel of H-MOR.

According to the H_2 chemisorption, EXAFS and *in-situ* CO-IR results, Pt clusters were found to be highly dispersed in Pt/H-MOR and Pt/H-Beta. The Pt particle size in Pt/H-MOR is smaller than that in Pt/H-Beta. Some of Pt clusters, however, remained isolated in the side-pockets of H-MOR and these metallic centers increased in population with the calcination temperature. In such a case, the metal/acid ratio in the main channel of H-MOR would decrease, so the selectivity to multibranched isomers should be low at high conversion. In addition, mordenite has one-dimensional pore structure with side-pockets at the wall of main channels, so if the platinum clusters in the main channel grow in size to fit the pore size of H-MOR during the reduction step, many of acid sites as well as platinum clusters located in the interior to the pore-plugging large clusters near the pore mouth would become inaccessible to the reactant and reaction intermediates. This supposition could be supported by the low hydrogenation activity of Pt/H-MOR compared to that of Pt/H-Beta.

On the other hand, zeolite Beta consists of intergrowth of linear channels (5.7×7.5 Å) of 12-MR and tortuous channels (6.5×5.6 Å) with channel intersections [Higgins et al., 1988]. Therefore, even if one of the channels are blocked by large particles (the linear channel might be blocked first),

reactant and reaction intermediates can have access to some of metal sites through the other channels. In conclusion, the metal/acid balance in Pt/H-Beta would be better than that in Pt/H-MOR even though the acid strength is lower and Pt particle size is larger than in Pt/H-MOR.

CONCLUSIONS

Platinum loaded large pore zeolites were tested for the hydroisomerization of *n*-hexane and *n*-heptane. The catalytic activity and the selectivity to multibranched isomers were found to be strongly dependent upon the distribution of acid and metal sites as well as the number of those sites in the bifunctional Pt/zeolite. The catalytic activity increased with the effective acidity probed by pyridine rather than with the total acidity probed by ammonia.

The selectivity to multibranched isomers was higher over Pt/zeolite with higher acid strength at low conversion. As the conversion increased, the metal/acid balance seemed to play an important role for high selectivity to multibranched isomers. The platinum particle size in Pt/H-MOR was much smaller than that in Pt/H-Beta. However, some of platinum particles remained isolated in the side-pockets of 8-MR and these metal sites increased in number as the calcination temperature increased. The hydrogenation activity of Pt/H-Beta was extremely high compared to Pt/H-MOR when the H/Pt values were identical in both catalysts. Among three different Pt-loaded zeolites, Pt/H-Beta showed the best performance for the hydroisomerization of *n*-paraffin by virtue of the proper metal/acid ratio in Pt/H-Beta in spite of the fact that the acid strength of H-Beta is much lower than that of H-MOR and H-Omega.

ACKNOWLEDGEMENT

The financial supports of SK Corp. and Korea Research Foundation (96-190) for this work are gratefully acknowledged. We also thank Professor R. Ryoo and Dr. S. J. Cho of the KAIST for their assistance during EXAFS data collection and analysis.

REFERENCES

Alvarez, F., Giannetto, G., Guisnet, M. and Perot, G., "Hydroisomerization and Hydrocracking of *n*-Alkanes. 2. *n*-Heptane Transformation on a Pt-Dealuminated Y Zeolites-Comparison with a Pt-Y Zeolite", *Appl. Catal.*, **34**, 353 (1987).

Buckermann, W. A., Huong, C. B., Fajula, F. and Gueguen, C., "^{27}Al MAS N.M.R. Evidence for the Reversible Transformation of the Coordination of Aluminum in Dealuminated Mazzite", *ZEOLITES*, **13**, 448 (1993).

Chmelka, B. F., Rosin, R. R., Went, G. T., Bell, A. T., Radke, C. J. and Petersen, E. E., "The Chemistry of Pt-NaY Zeolite Preparation", *Stud. Surf. Sci. Catal.*, **49**, 995 (1989).

Folefoc, G. N. and Dwyer, J., "Dispersion of Platinum in Pt/ZSM-5 Zeolites", *J. Catal.*, **136**, 43 (1992).

Giannetto, G. E., Perot, G. R. and Guisnet, M. R., "Hydroisomerization and Hydrocracking of *n*-Alkanes. 1. Ideal Hydroisomerization PtHY Catalysts", *Ind. Eng. Chem. Prod. Res. Dev.*, **25**, 481 (1986).

Guisnet, M. R. and Perot, G. R., in "Zeolite: Science and Technology" (Ribeiro, F. R., Rodrigues, A. E., Rollmann, L. D., Naccache, C., Eds.), Martinus Nijihoff, Hague, 397 (1984).

Higgins, J. B., LaPierre, R. B., Schlenker, J. L., Rohrman, A. C., Wood, J. D., Kerr, G. T. and Rohrbaugh, W. J., "The Framework Topology of Zeolite Beta", *ZEOLITES*, **8**, 446 (1988).

Homeyer, S. T. and Sachtler, W. M. H., "Elementary Steps in the Formation of Highly Dispersed Palladium in NaY 2. Particle Formation and Growth", *J. Catal.*, **118**, 266 (1989).

Klinowski, J. and Anderson, M. W., "A High-resolution Solid-state Nuclear Magnetic Resonance Study of the Ordering of Silicon and Aluminum in Synthetic Mazzite (Zeolite Omega)", *J. Chem. Soc. Faraday Trans* 1, **82**, 569 (1986).

Lee, J. K., Lee, H. T. and Rhee, H. K., "Isomeriztion of *n*-Hexane over Platinum Loaded Zeolites", *React. Kinet. Catal. Lett.*, **57**(2), 323 (1996).

Lee, J. K. and Rhee, H. K., "Characteristics of Pt/H-Beta and Pt/H-Mordenite Catalysts for the Isomerization of *n*-Hexane", *Catal. Today*, **38**, 235 (1997).

Leu, L.-J., Hou, L.-Y., Kang, B.-C., Li, C., Wu, S.-T. and Wu, J.-C., "Synthesis of Zeolite β and Catalytic Isomerization of *n*-Hexane over Pt/H-β Catalysts", *Appl. Catal.*, **69**, 49 (1991).

Massiani, P., Chauvin, B., Fajula, F. and Figueras, F., "Activation of Zeolite Ω 1. Physicochemical Characterization of Calcined and Self-Steamed Samples", *Appl. Catal.*, **42**, 105 (1988).

Maxwell, I. E. and Stork, W. H. J., "Hydrocarbon Processing with Zeolites", *Stud. Surf. Sci. Catal.*, **58**, 571 (1990).

Mortier, W. J., "Temperature-Dependent Cation Distribution in Dehydrated Calcium-Exchanged Mordenite", *J. Phys. Chem.*, **81**(3), 1334 (1997).

Nicolas, S., Massiani, P., Vera Pacheco, M., Fajula, F. and Figueras, F., "A New Synthesis Route to Zeolite Omega", *Stud. Surf. Sci. Catal.*, **37**, 115 (1988).

Otten, M. M., Clayton, M. J. and Lamb, H. H., "Platinum-Mordenite Catalysts for *n*-Hexane Isomerization: Characterization by X-Ray Absorption Spectroscopy and Chemical Probes", *J. Catal.*, **149**, 211 (1994).

Shpiro, E. S., Joyner, R. W., Minachev, K. M. and Pudney, P. D. A., "Structural Studies of Platinum/ZSM-5 Catalysts", *J. Catal.*, **127**, 366 (1991).

Stakheev, A. Yu., Shpiro, E. S., Tkachenko, O. P., Jaeger, N. I. and Schulz-Ekloff, G., "Evidence for Monatomic Platinum Species in H-ZSM-5 from FTIR Spectroscopy of Chemisorbed CO", *J. Catal.*, **169**, 382 (1997).

Wadlinger, R. L., Kerr, G. T. and Rosinski, E. J., *U.S. Patent* 3,308,069 (1967).

Zholobenko, V. L., Lei, G.-D., Carvill, B. T., Lerner, B. A. and Sachtler W. M. H., "Identification of Isolated Pt Atoms in H-Mordenite", *J. Chem. Soc. Faraday Trans.*, **90**(1), 233(1994).